

Non-Isothermal Kinetics of Crystallization and Phase Transformation of $\text{SiO}_2\text{-Al}_2\text{O}_3\text{-P}_2\text{O}_5\text{-CaO-CaF}_2$ Glass

Bogdan Il. Bogdanov, Plamen S. Pashev, Yancho H. Hristov, Dimitar P. Georgiev, Irena G. Markovska

Abstract—The crystallization kinetics and phase transformation of $\text{SiO}_2\text{-Al}_2\text{O}_3\text{-0,56P}_2\text{O}_5\text{-1,8CaO}\cdot\text{0,56CaF}_2$ glass have been investigated using differential thermal analysis (DTA), x-ray diffraction (XRD), and scanning electron microscopy (SEM). Glass samples were obtained by melting the glass mixture at $1450^\circ\text{C}/120$ min. in platinum crucibles. The mixture were prepared from chemically pure reagents: SiO_2 , $\text{Al}(\text{OH})_3$, H_3PO_4 , CaCO_3 and CaF_2 . The non-isothermal kinetics of crystallization was studied by applying the DTA measurements carried out at various heating rates. The activation energies of crystallization and viscous flow were measured as $348,4 \text{ kJ}\cdot\text{mol}^{-1}$ and $479,7 \text{ kJ}\cdot\text{mol}^{-1}$ respectively. Value of Avrami parameter $n \approx 3$ correspond to a three dimensional of crystal growth mechanism. The major crystalline phase determined by XRD analysis was fluorapatite ($\text{Ca}(\text{PO}_4)_3\text{F}$) and as the minor phases – fluormargarite ($\text{CaAl}_2(\text{Al}_2\text{SiO}_2)_{10}\text{F}_2$) and vitlokite ($\text{Ca}_9\text{P}_6\text{O}_{24}$). The resulting glass-ceramic has a homogeneous microstructure, composed of prismatic crystals, evenly distributed in glass phase.

Keywords—glass-ceramic, crystallization, non-isothermal kinetics, Avrami parameter

I. INTRODUCTION

WITH the advent of modern era and with the development of medical science the living of people around the globe has changed a lot. Bioceramics has a major role to play in the field of repair and reconstruction of diseased, damaged or worn out parts of the body. Bioceramics are produced in a variety of forms and phases and serve many different functions of the body. The bioactive glass was first produced by Hench et al in 1969 which can bond chemically to the bone. Since then a lot of research has undergone for the development of biomaterials. [1] The main achievements in glass production is the design of bioactive glass materials and a lot of research is being carried out around the globe for improving its properties to make it as biocompatible as possible. To make the material biocompatible so that it can interact with the living tissue there should be formation of apatite phase which is a part of natural bone and provides strength and growth ability. [2 - 4]

B. Il. Bogdanov - Department of inorganic substances and silicates, Assen Zlatarov University, 1 Prof. Yakimov Str., 8010 Bourgas, Bulgaria, e-mail: bogdanov_b@abv.bg

P.S. Pashev- Department of inorganic substances and silicates, Assen Zlatarov University, 1 Prof. Yakimov Str., 8010 Bourgas, Bulgaria.

Y. H. Hristov - Department of Material science and technology, Assen Zlatarov University, 1 Prof. Yakimov Str., 8010 Bourgas, Bulgaria, e-mail: janchrist@abv.bg

Dimitar P. Georgiev - Department of Material science and technology, Assen Zlatarov University, 1 Prof. Yakimov Str., 8010 Bourgas, Bulgaria, e-mail: dgeorgiev@btu.bg

I. G. Markovska - Department of inorganic substances and silicates, Assen Zlatarov University, 1 Prof. Yakimov Str., 8010 Bourgas, Bulgaria, e-mail: imarkovska@abv.bg

The A/W glass-ceramic studied by Kokubo in 1980 shows high bioactivity and high mechanical strength compared to other glasses and glass-ceramics which is due to the relatively high fracture toughness due to the precipitation of β -wollastonite in addition to apatite. Crystallisation of the parent glass in a bulk form led to the occurrence of large cracks in the crystallised sample while crystallisation of the same glass in a powder compact led to the formation of a crack-free dense crystallised sample due to uniform crystallization of apatite and wollastonite as demonstrated by Kokubo et al. [5,6]

For the improved mechanical properties and machineability controlled crystallization of both mica and apatite can be carried out. Desired bioactivity is taken care by apatite formation and machinability by mica phase. The special characteristic of the glass-ceramic was that two distinct crystal phases were precipitated in parallel: apatite and mica were produced simultaneously with a volume nucleation mechanism. The resultant glass ceramic gives high value of mechanical properties. [7]

Fluormica glass-ceramics shows a favorable combination of thermal, electrical and biomedical properties which can be easily cut, drilled and turned with conventional tools. Laminated structure of mica crystals is, directly responsible for the desirable machinability because they cleave easily along the interfaces between layers while being machined. [8 - 10]

In this study, we studied the crystallization kinetics of $\text{SiO}_2\text{-Al}_2\text{O}_3\text{-P}_2\text{O}_5\text{-CaO}$ glass system. CaF_2 was added to glass composition to improve some properties such as chemical resistance of the glass-ceramic system. [2]

II. EXPERIMENTAL AND METHODS

The $\text{SiO}_2\text{-Al}_2\text{O}_3\text{-0,56P}_2\text{O}_5\text{-1,8CaO}\cdot\text{0,56CaF}_2$ glass was melted from reagent grade SiO_2 , $\text{Al}(\text{OH})_3$, H_3PO_4 , CaCO_3 and CaF_2 . The bioglass sample has the following composition (by weight): SiO_2 15%, Al_2O_3 25,3%, CaO 25%, P_2O_5 21,1% and CaF_2 13,6%. All samples obtained in 50 to 100 g batches of the desired composition were accurately weighed and well premixed. The batches were transferred into a platinum crucible and melted at 1450°C in an electric furnace (Naber) for 2 h. After that, the molten glass was cast into preliminarily heated graphite dies. The tempering was carried out at 680°C for 12 h, followed by free cooling of the oven.

Differential thermal analysis was conducted in the temperature range of 25 to 1000°C . The 200 mg powder samples ($>67 \mu\text{m}$) were heated in air at rates of 5, 10, 15, and $20^\circ\text{C}/\text{min}$ by the derivatograph OD-102 (MOM, Hungary). Al_2O_3 powder was used as the reference material.

The X-ray analyses were carried out by the method of powder diffraction using X-ray apparatus equipped with goniometer URD-6 (Germany) with cobalt anode and $K\alpha$ emission.

Tesla BS 340 (Czech Republic) scanning electron microscope was used to examine the surface of the polished samples, etched (5 parts HF, 2 parts HCl, and 93 parts H₂O) and coated with a thin gold film.

III. RESULTS AND DISCUSSION

A. Differential thermal analysis and crystalline phases

The DTA curves of the glasses are presented in Fig. 1. Endothermic reactions at the temperature range of 792–821°C have been identified. These endothermic peaks are attributed to the glass transition (T_g), at which the sample changes from solid to liquid behaviour. Various exothermic effects such as that at 867–899°C indicating reaction of crystallization in the glasses are also recorded.

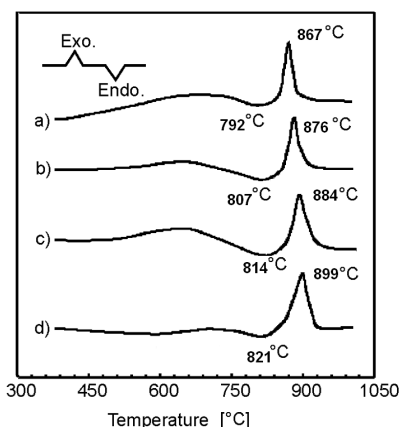


Fig. 1 DTA diagrams of the $\text{SiO}_2\text{-Al}_2\text{O}_3\text{-}0,56\text{P}_2\text{O}_5\text{-}1,8\text{CaO}\text{-}0,56\text{CaF}_2$ glass at the heating rates of a) 5 °C/min, b) 10 °C/min, c) 15 °C/min and d) 20 °C/min

The appearance of a crystallization peak on the DTA curve implies that at least a different crystal phase is formed during the heat treatment. The major crystalline phase (900°C/60 min.) determined by XRD analysis was fluorapatite ($\text{Ca}(\text{PO}_4)_3\text{F}$) and as the minor phases – fluormargarite ($\text{CaAl}_2(\text{Al}_2\text{SiO}_2)_{10}\text{F}_2$) and vitlokite ($\text{Ca}_9\text{P}_6\text{O}_{24}$).

SEM micrograph of the polished surface of the glass-ceramics is shown in Fig. 2. Prismatic crystals characteristic for apatite structure are shown in [2]. They, 10–20 μm in size, were evenly distributed throughout the native glass phase. Crystals of different habitus were also observed due to the presence of alloyed phases. Their sizes were in the range 5–10 μm.

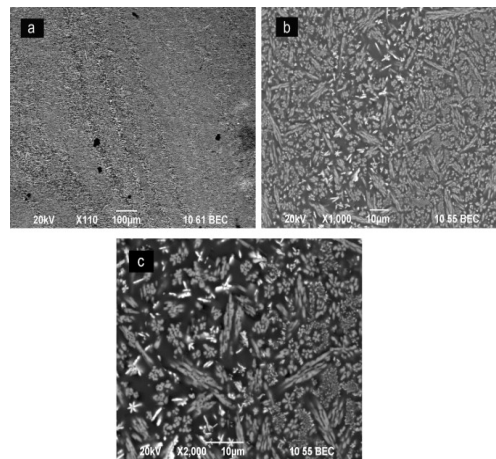


Fig. 2 SEM micrographs of glass-ceramic samples at magnifications: (a) ×110, (b) ×1000, (c) ×2000

B. The kinetics of crystallization

Solid state reactions such as crystallization of glass can be described by the phenomenological Johnson–Mehl–Avrami (JMA) equation [12, 13, 14].

$$X = 1 - \exp[-(kt)^n] \quad (1)$$

Taking natural logarithms and rearranging Eq. (1), we obtain

$$\ln(1 - X) = n \ln k + n \ln t \quad (2)$$

where X is the volume fraction crystallized after time t , n is the Avrami parameter which depends on the growth direction number and the mechanism of nucleation and crystal growth [15] and k is the reaction rate constant [s^{-1}] whose temperature dependence being expressed by the Arrhenius equation:

$$k = V \exp(-E_a/RT) \quad (3)$$

where V is the frequency factor [s^{-1}], E_a – the activation energy for crystallization [$\text{J}\cdot\text{mol}^{-1}$], R – the gas constant and T – the absolute temperature [K].

From the value of the activation energy E_a , the Avrami parameter n can be calculate by the DTA results [12, 13, 16]:

$$n = \frac{2.5}{\Delta T} \frac{T_p^2}{(E_a/R)} \quad (4)$$

where ΔT is the full width of the exothermic peak at the half maximum intensity from DTA crystallization peak.

The value of the activation energy for crystallization of glasses was determined using a method based on JMA equation which was first introduced by Kissinger and modified by others. This method is based on the dependence of the crystallization peak temperature (T_p) on the DTA heating rate (β) [12, 13, 15–17]:

$$\ln \frac{T_p^2}{\beta} = \ln \frac{E_a}{R} - \ln V_a + \frac{E_a}{RT_p} \quad (5)$$

likewise, Eq. (5) can also be used to predict the viscous energy [12, 13]:

$$\ln \frac{T_g^2}{\beta} = \ln \frac{E_c}{R} - \ln V_c + \frac{E_c}{RT_g} \quad (6)$$

where E_c is the corresponding activation energy for viscous flow, T_g is the glass transformation temperature, V_a is the frequency factor for crystallization and V_c is the frequency factor for viscous flow.

Plots of $\ln(T_p^2/\beta)$ vs. $1/T_p$ and $\ln(T_g^2/\beta)$ vs. $1/T_g$ obtained at various heating rates should be linear with the slopes E_a/R and the intercepts $\ln(E_a/R) - \ln V_a$ and $\ln(E_c/R) - \ln V_c$. Therefore, if E_a/R and E_c/R are estimated from the slope, the frequency factors can be calculated from the intercepts. The same data are plotted in figs. 3 and 4.

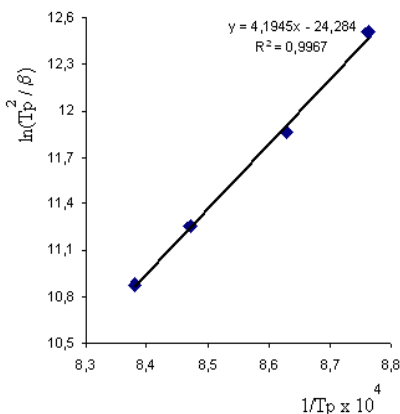


Fig. 3 Plot of $\ln(T_p^2/\beta)$ vs. $1/T_p$ for the determination of the activation energy for the crystallization of $\text{SiO}_2.\text{Al}_2\text{O}_3.0,56\text{P}_2\text{O}_5.1,8\text{CaO}.0,56\text{CaF}_2$ glass

In accordance with the literature data, the temperature corresponding to the crystallization peak is higher at faster heating rates [12]. The calculated values of E_a , E_c and V_a, V_c (Figs. 3 and 4) are as follows: $E_a=348,4$ kJ/mol, $E_c = 479,7$ kJ/mol, $V_a = 1,24 \times 10^{15} \text{ s}^{-1}$, $V_c = 6,32 \times 10^{17} \text{ s}^{-1}$.

The n values, calculated from Eq. (4), are given in Table 1. It can be seen that $n \approx 3$ and $n > 3$, which indicates that the crystallization of the $\text{SiO}_2.\text{Al}_2\text{O}_3.0,56\text{P}_2\text{O}_5.1,8\text{CaO}.0,56\text{CaF}_2$ glass at all heating rates is caused by bulk nucleation with three dimensional crystal growth.

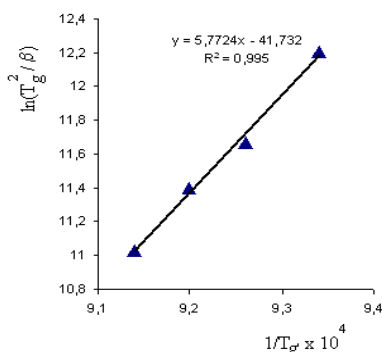


Fig. 4 Plot of $\ln(T_g^2/\beta)$ vs. $1/T_g$ for the determination of the activation energy for the viscous flow of $\text{SiO}_2.\text{Al}_2\text{O}_3.0,56\text{P}_2\text{O}_5.1,8\text{CaO}.0,56\text{CaF}_2$ glass

TABLE I
THE n VALUES OF $\text{SiO}_2.\text{Al}_2\text{O}_3.0,56\text{P}_2\text{O}_5.1,8\text{CaO}.0,56\text{CaF}_2$ GLASS

| Heating rate, β [K·min ⁻¹] | 5 | 10 | 15 | 20 |
|---|-----|-----|-----|-----|
| n | 3,1 | 2,9 | 3,0 | 2,7 |

IV. CONCLUSIONS

In the crystallization of the $\text{SiO}_2.\text{Al}_2\text{O}_3.0,56\text{P}_2\text{O}_5.1,8\text{CaO}.0,56\text{CaF}_2$ glass, fluorapatite ($\text{Ca}(\text{PO}_4)_3\text{F}$), fluormargarite ($\text{CaAl}_2(\text{Al}_2\text{SiO}_5)_2$) and vitlokite ($\text{Ca}_9\text{P}_6\text{O}_{24}$) crystallize. The Johnson–Mehl–Avrami and Kissenger equations were used to calculate the activation energies of crystallization and of viscous flow. The dimensionless parameter n , related to the reaction mechanism was determined by using T values obtained from DTA measurements at various heating rates.

Depending on the heating rate, the n values varied between 2,7 and 3,1, indicating the bulk nucleation in the $\text{SiO}_2.\text{Al}_2\text{O}_3.0,56\text{P}_2\text{O}_5.1,8\text{CaO}.0,56\text{CaF}_2$ glass by three-dimensional crystal growth.

The activation energies of the crystallization and of viscous flow were calculated as 348 kJ mol⁻¹ and 479 kJ mol⁻¹, respectively.

ACKNOWLEDGMENT

The authors would like to acknowledge for the financial support provided by Bulgarian Ministry of Education and Science, Fund “Scientific Investigation”.

REFERENCES

- [1] “An introduction to Bioceramics” by Larry L. Hench & June Wilson, World Scientific publication, Singapore.
- [2] B.I. Bogdanov, P.S. Pashev, J.H. Hristov, I.G. Markovska, “Bioactive fluorapatite-containing glass ceramics”, *Ceramics International*, 35, (2009), 1651–1655.
- [3] W. Holand, V. Rheinberger, E. Apel, C. van’t Hoen, M. Hoeland, A. Dommann, M. Obrecht, C. Mauth, U. Graf-Husner, Clinical applications of glass-ceramics in dentistry, *J. of Mater. Sci. – Mater. Med.*, 17, (2006), 1037–1042.
- [4] C.O. Freeman, I.M. Brook, A. Johnson, P.V. Hatton, K. Stanton, “Crystallization modifies osteoconductivity in an apatite-mullite glass-ceramic”, *Jour. of Mater. Sci. – Mater. Med.*, 14, (2003), 985–990.
- [5] Valeria Cannillo, Fiorenza Pierli, Sanjay Sampath, Cristina Siligardi, “Thermal and physical characterisation of apatite/wollastonite bioactive glass-ceramics”, *Journal of the European Ceramic Society*, 29, (2009), 611–619.
- [6] Kokubo, T., Ito, S., Sakka, S. and Yamamuro, T., Formation of a high strength bioactive glass-ceramic in the system MgO–CaO–SiO₂–P₂O₅. *Journal of Materials Science*, 21, 1986, 536–540.
- [7] Wolfram Holand, “Glass-ceramics Biocompatible and bioactive glass-ceramics - state of the art and new directions”, Section 3, *Journal of Non-Crystalline Solids*, 219, (1997), 192–197.
- [8] W. Vogel, W. Holand K. Naumann, J. Gummel, “Development Of Machineable Bioactive Glass Ceramics For Medical Uses”, *Journal of Non-Crystalline Solids*, 80, (1986), 34–51.
- [9] B. Ashouri Rad, P. Alizadeh, “Pressureless sintering and mechanical properties of SiO₂–Al₂O₃–MgO–K₂O–TiO₂–F (CaO–Na₂O) machinable glass-ceramics”, *Ceram. International*, 35, (2009), 2775–2780.
- [10] D.S. Baik, K.S. No, J.S. Chun, Y.J. Yoon, Mechanical properties of mica glass-ceramics, *Journal of the American Ceramic Society*, 78, (5), (1995), 1217–1222.
- [11] Demirkesen E., Goller G., Effect of Al₂O₃ additions on the acid durability of a Li₂O–ZnO–SiO₂ glass and its glass-ceramic, *Ceramics Int.*, 29, (2003), 463.
- [12] Yilmaz S., Ozkan O.T., Gunay V., Crystallization kinetics of basalt glass, *Ceramics Int.*, 22, (1996), 477.
- [13] Bayrak G., Yilmaz S., Crystallization kinetics of plasma sprayed basalt coatings, *Ceramics Int.*, 32, (2006), 441.
- [14] Balaya P., Sunandana C.S., Crystallization studies of 30Li₂O–70TeO₂, *J. Non-Cryst. Sol.*, 162 (1993), 253.
- [15] Karamanov A., Pelino M., Crystallization phenomena in iron-rich glasses, *J. Non-Cryst. Sol.*, 281, (2001), 139.
- [16] Park J., Heo J., Nucleation and crystallization kinetics of glass derived from incinerator flu ash waste, *Ceramics Int.*, 28, (2002), 669.
- [17] Erol M., Kucukbayrak S., Mericboyu A.E., Ovecoglu M.L., Crystallisation behaviour of glasses produced from flyash, *J. Europ. Cer. Soc.*, 21, (2001), 2835.